Articles                                    Department of Plant, Soil, and Agricultural Systems

# Measurement of granular flow in a vertical column using pulse induction (PI)

Nasreddine Meziane
*University of Sciences and Technology of Oran Mohamed Doudiaf*

Ahmed Bettahar
*University Hassiba Ben Bouali of Chief*

Ruplal Choudhary
*Southern Illinois University Carbondale*, choudhry@siu.edu

Dennis G. Watson
*Southern Illinois University Carbondale*, dwatson@siu.edu

Follow this and additional works at: http://opensiuc.lib.siu.edu/psas_articles

### Recommended Citation

Measurement of granular flow in a vertical column using pulse induction (PI)

Nasreddine Meziane[a], Ahmed Bettahar[b], Ruplal Choudhary[c,*], Dennis G. Watson[c]

[a] Mechanics Department, Faculty of Mechanical Engineering, University of Sciences and Technology of Oran Mohamed Boudiaf, Algeria
[b] Mechanics Department, Faculty of Sciences, University Hassiba Ben Bouali of Chlef, Algeria
[c] Department of Plant, Soil and Agricultural Systems, 1205 Lincoln Dr, MC 4415, Southern Illinois University, Carbondale, IL 62901, USA
*Corresponding Author: choudhry@siu.edu; Tel: 618 453 6985

**Abstract**
Gravity flow of granular materials in vertical columns can generate pressure and density fluctuations which are difficult to quantify. Examination of prior research led us to propose a new measurement technique based on the principle of pulse induction (PI) for metal detection. An experimental device using 8 mm diameter spherical particles flowing through a polyvinylchloride (PVC) pipe of 75 mm diameter and 1000 mm height was developed to demonstrate the feasibility of PI. Ten PI coils were used to quantify tracer movement through the column with time. Average and instantaneous velocities were determined for five diameters of outlet orifices: 68.0, 62.5, 54.5, 44.0 and 36.5 mm. Flow rate was calculated and modelled. When compared to prior research, PI proved to be a reliable method for flow measurement in opaque ducts.
**Key words:** flow of granular materials, emptying silo, pulse induction, PI, tracer, velocity, mass flow.

**Nomenclature**
**Symbols**

| | |
|---|---|
| $\phi$ | porosity |
| $\rho_a$ | bulk density of bead, kg m$^{-3}$ |
| $\rho_s$ | solid density of bead, kg m$^{-3}$ |
| $A$ | area of horizontal cross section of the column, cm$^2$ |
| $a$ | proportionality of coefficient |
| $C_b$ | a dimensionless constant |
| $D$ | diameter to outlet opening, mm |
| $D_{Ci}$ | interior diameter of a vertical column, mm |
| $Dp_{d\text{max.}}$ | maximum of average depth of detection, mm |
| $Dp_{di}$ | depth of detection of rank i |
| $d$ | diameter of bead, mm |
| $E_h$ | 95% confidence interval of height, mm |
| $E_Q$ | 95% confidence interval of mass flow rate, kg s$^{-1}$ |
| $E_t$ | 95% confidence interval of time, s |
| $E_v$ | 95% confidence interval of velocity, mm s$^{-1}$ |
| $e$ | thickness of a vertical column, mm |
| $g$ | gravitational acceleration, its magnitude, equal to 9.81, m s$^{-2}$ |
| $h_c$ | height of the cone, cm |
| $h_d$ or $h$ | height of detection, cm |
| $h_{10}$ | slice of granular material between zero depth and the lowest PI coil (rank 10) |
| $k$ | empirical dimensionless |
| $L$ | length of a vertical column, cm |

| $m$ | unit mass, g |
| --- | --- |
| $n$ | exponent |
| $Q$ | average mass flow, kg s$^{-1}$ |
| $R^2$ | coefficient of determination |
| $t$ | time, s |
| $t_{10}$ | maximum of average time elapsed to travel through the $h_{10}$, s |
| $v$ | velocity of trace, m s$^{-1}$ |
| $v_{mean}$ | average velocity of the tracer, m s$^{-1}$ |

Abbreviations

| CCD | charged coupled device |
| --- | --- |
| ID | inside diameter |
| MRI | magnetic resonance imaging |
| PI | pulse induction |
| PVC | polyvinylchloride |
| TM | task manager |
| DT | detector |
| TI | timers |

## 1. Introduction

Granular flows pose many problems in industry (Duran, 1997). Industries such as agriculture, food processing, pharmaceuticals, cosmetics and building construction are among the large-scale users of granular materials (Duran, 1997; Mitarai & Nori, 2006; Jaeger & Nagel, 1992). When emptying vertical columns (silos) by gravity, material arching and other phenomena may occur which impede or block the flow of ensiled material at the outlet (Jackson, 2000). In these cases, flow may become inconsistent leading to density waves or strong pressure gradients, disrupting the flow of grain which may damage pipelines (Reydellet, Rioual, Clement 2000; Wang, Jackson, Sundaresan, 1997). The flow of granular materials in silos, obeys complex dynamics that can generate problems such as high pressure and density fluctuations during emptying (Andrade, Trevino, Medina, 1996). These flows generate several phenomena which are difficult to quantify with existing flow measurement devices.

The most commonly adopted approach in determining granular material flow is the use of tracers that move with the material. These tracers can be followed either visually or by means of detection equipment. The radio beacon method is a technique that uses radio frequency transmitters (size ~ 70 mm). The transmitters are placed at different predetermined locations within the granular material during filling. Since the position of each transmitter within the silo is known and the time required for each transmitter to reach the outlet is measured, the average velocity for each transmitter can be calculated (Ooi, Chen, Rotter, 1998; Ooi & Rotter, 1998). This method does not provide any details on whether a particular transmitter moves at a relatively constant speed or if it has considerable velocity changes as it flows to the silo outlet. The direct visualisation method determines velocity fields from digital images (Medina, Andrade, Trevino, 1998; Chou, Hsu, Lau, 2002) or by using spatiotemporal diagrams obtained with a CCD (charged coupled device) camera (Degouet, 2005; Bertho, 2003). This method quantifies the velocity of the beads in contact with the wall or that of the free surface. Degouet (2005) used a micro impulse technique to quantify the position and vertical velocity at the centre of the free surface of a granular material in a column of measurement, but access to the velocity at other points of the volume was not feasible. Magnetic resonance imaging (MRI) has been used to measure grain flow (Chevoir et al., 2001). MRI was used to quantify the velocity profile in a 54 mm diameter tube. The 1.3 mm diameter mustard seed materials used for this study were rich in protons and particularly well suited to this approach.

The pulse induction (PI) metal detection method relies on the electrical conductivity of metal objects. The sensitivity of a PI detector is determined primarily by the current in the search coil. The PI method of detection works by subjecting objects to a rapidly changing electromagnetic field. The field is produced by building up a current in a simple multi-turn search coil, and then forcing the current to fall very rapidly by switching off the supply. A metal object within the electromagnetic field generates a Foucault (or eddy) current. As soon as the excitation terminates, the Foucault current decays to a value of zero. These Foucault currents induce a magnetic field, typically a few mV to less than 1μV, which is measured by the detector during the detection phase (Stuart, 1994; Crone & Crone, 1989; Guelle, Smith, Lewis & Bloodworth, 2003).

The limitations of prior methods of measuring gravitational flow within a vertical column led us to test a new measurement technique based on the principle of metal detection by PI. The objectives of this study were to: (1) test the PI technique for measuring the coupled time-height of a tracer at different points of a vertical granular flow using different outlet diameters, and (2) compare the experimental results provided by the PI method with those from other experimental results reported in literature. Data obtained by PI were expected to lead to enhanced understanding of physical phenomena caused by gravitational flow of grains in vertical columns.

## 2. Materials and Methods

### *2.1 Description of the experimental device*
In complement to the available techniques of velocity measurements, an experimental device was designed and constructed to measure the time evolution of the height of the tracer initially placed in the centre of a free surface of granular volume. A schematic diagram of the experimental device is shown in Fig. 1a. It consisted of a vertical column made of an opaque PVC pipe with interior diameter (ID) $D_{Ci}$= 75 mm, of thickness e = 2.5 mm and of length L = 1000 mm. The outlet diameter ($D$) at the bottom of the column was varied with a set of five cones ranging from 36.5 to 68.0 mm ID (see Table 1). An open space was provided between the bottom of the outlet and a bucket to collect the granular material. This open space allowed visual observation of the material movement (continuous or interrupted) and flow rate (Lubert, 2000).

A mechanism was needed to rapidly open the outlet at the bottom of the column to minimize the effect on flow conditions while the outlet was being opened to full diameter. Degouet (2005) used a plastic valve at the bottom of hopper to allow rapid opening. Bertho (2003) used a screw placed horizontally at the outlet of the tube to regulate the flow of glass beads. The flow conditions were influenced by those opening devices. For this study, a sectorial design was implemented for an obturating valve (or obturator) (see Fig. 1b & c). The obturator was operated by an electrically controlled, mechanical device (similar to that which operates the tray of a compact disk drive) to minimise opening time.

Electronics modules were constructed to implement PI, control, and timer circuitry for the experimental device. The PI circuit is based on Crone and Crone (1989). The column was equipped with 10 PI detection coils, placed at different predetermined heights, starting just below the fill height and ending above the outlet cone, before the transition to funnel flow. Each coil had an ID of 80 mm and consisted of 35 turns of 0.5 mm copper conductor and was supplied with 12 V dc, generating an inductance of approximately 0.25 mH. An elastic band was attached to each coil to hold it in place on the column. The detector module (DT) (see Fig. 1a) contained the PI circuit for a single PI coil and was supplied by 15 V dc. The task manager (TM) module was designed to control opening the obturator, switch DT power to

each of the 10 PI coils, and control the timers (TI). The TM operated with a 12 V dc power supply. The bank of timers (TI) consisted of eleven Kadio KD-611A (Putian Dexing Electronic Company Limited, Putian, Fujian, China) timers with a precision of 0.01 s. One timer was designated as the start-up timer and corresponded to the fill height of granules in the column. Each of the other 10 times corresponded with a different PI coil. The start/stop and reset switches of each timer were controlled by the TM.

### 2.2 Granular material
The granular particles used for this study were beads of uniform size and shape (diameter $d$ = 7.91 ± 0.07 mm with average unit mass m = 0.22 ± 0.012 g). The beads were solid, plastic spheres with a smooth exterior surface and a diametrically positioned hole. These beads had solid density $\rho_s$ = 840.34 ± 45.84 kg m$^{-3}$ and bulk density $\rho_a$ = 562.04 ± 30.71 kg m$^{-3}$. When the column was full and at static condition, the average porosity was $\phi$ = 0.33, based on the equation:

$$\phi = \frac{\rho_s - \rho_a}{\rho_s} \tag{1}$$

Where $\rho_s$ is solid density of a bead and $\rho_a$ is bulk density. One bead of same size, but contrasting colour was selected for the tracer. A metal strand (terminal extracted from a chemical capacitor) of 0.9 mm diameter and 8 mm length was inserted into the existing diametrical hole in the tracer bead and secured with adhesive. The smooth exterior surface of the bead was maintained. The total mass of the tracer (metal strand + bead) was approximately 0.3 g. For experimental purposes, it was assumed that the velocity of the tracer was the same as other beads on the same horizontal plane as the tracer.

### 2.3 Measurement of actual depth of tracer at time of detection by each PI coil
The actual depth of the tracer was measured within the column at the point of detection by each PI coil. This calibration was performed within the column in the absence of the granular mass. For each PI coil, the tracer was suspended by an inextensible wire into the column until it was detected by the respective coil. This process was repeated 20 times and each time the length of the wire from the tracer to a fixed point at the top of the column was measured and then compared to a 1000 mm graduated ruler. For each coil of rank $i$, the actual depth of the tracer at the respective coil was the difference between the maximum depth of detection $Dp_{d\max}$ (coil of rank 10) and the depth of detection at coil of rank $i$ was $Dp_{di}$.

### 2.4 Measurement of tracer path time
For each outlet diameter tested, the column was loaded with the same granular material, and the same tracer was placed in the centre of the free surface. An experimental run was initiated by the operator activating a button on the TM. The TM reset all timers to zero and simultaneously opened the obturator, started the start-up timer, and directed DT power to the top PI coil (Coil 1). Once Coil 1 detected the tracer, the corresponding timer (Timer 1) was started and DT power was switched to Coil 2. When Coil 2 detected the tracer, the corresponding timer (Timer 2) was started and DT power was switched to Coil 3. This process repeated until Coil 10 detected the tracer and Timer 10 was started. Once granular flow stopped, the operator pressed a button on the TM which caused all timers to stop. Data from the start-up and the other 10 timers were recorded. The procedure was repeated for a total of 20 sets of observations for each outlet size.

### 2.5 Data summary and calculations
For each experimental run, the time displayed on each timer was subtracted from the start-up timer to calculate the time elapsed between the start-up timer and the tracer reaching each PI coil. For each outlet size, the mean and standard deviation of elapsed time at each PI coil were calculated from the 20 observations. The instantaneous vertical velocity of the tracer at each PI coil was calculated based on

the time and distance from the prior PI coil. The average vertical velocity was calculated using the trapezoidal rule.

The average mass flow of the granular material in the column was calculated using two methods. The first method expressed by Eq. (2) is an indirect measure and is based on measuring the mass of granular material travelled between the time of the start-up timer (zero depth) and the timer corresponding to the lowest PI coil (rank 10).

$$Q = \rho_a \frac{A h_{10}}{t_{10}}$$
(2)

where $Q$ is mass flow, $\rho_a$ is the apparent bulk density of granular material, A is the area of horizontal cross section of the column, $h_{10}$ is the slice of the granular material between zero depth (free surface) and the rank 10 PI coil, and $t_{10}$ is the emptying time of the slice $h_{10}$. The second method expressed by Eq. (3) is also an indirect method. It is based on the calculation of the average velocity of tracer between the start-up instance and detection at PI coil rank 10, with the assumption that the individual velocity of the tracer approximates those of small agglomerates lying on the same horizontal plane. The average mass flow rate of bulk of particles may be given by

$$Q = \rho_a v_{mean} A$$
(3)

where $v_{mean}$ is the average velocity of the tracer. Results of Eqs. (2) and (3) tend to diverge as outlet diameter increases. The mass flow rates calculated by Eqs. (2) and (3) for each outlet diameter were fitted to an expression of power type

$$Q = a D^n$$
(4)

Where $a$ and $n$ are empirical constants and $D$ is the outlet diameter. Beverloo et al. (1961) provided a better correlation of mass flow rate $Q$ of granular material through an outlet opening of diameter $D$, as shown in Eq. (5).

$$Q = C_b \rho_a \sqrt{g} (D - (k d))^n$$
(5)

where $C_b$ is a dimensionless constant depending primarily on the geometrical characteristics of the silo, and $k$ is an empirical dimensionless constant which depends on the shape of the particles and acceleration due to gravity ($g$), and $d$ is mean particle diameter. Beverloo et al. (1961) gave the values for $k$, $n$ and $C_b$ as 1.4, 2.5 and 0.58 respectively. Later, Le Pennec et al. (1995) gave the value for $k$ as 1.5 for spherical particles and slightly higher values for the angular particles.

The mass flow rates obtained by Eqs. (2) or (3) as a function of the outlet diameter were adjusted according to the Eq. (5) whose exponent $n$ was obtained by the minimization of residual sum of squares (SSR). The coefficient of determination ($R^2$) was used to express the part of dispersion explained by a model.

## 3. Results and Discussion

### 3.1 Effect of orifice size on time evolution of tracer height
The actual depth of the tracer as recorded at each PI coil for each outlet diameter had an average variance of 1.1 mm or 0.5% with a range of 0.6 to 2.6 mm. This was considered suitable repeatability for this study. Table 2 summarises the mean time (s) from start-up timer to each timer corresponding to a PI coil. The average standard deviation was 0.05 s with a range of 0.02 to 0.19 s. For each outlet size, the

mean time recorded for each PI coil was used to quantify the time-height change of the tracer (see Fig. 3). As expected, the time between PI coils increased with a decrease in outlet size. The curves obtained have the same tendency as those obtained by Steingart and Evans (2005) and Degouet (2005).

### 3.2 Velocity of particles

The mean velocities of the tracer are summarized in Table 3. Instantaneous vertical velocities of the tracer were calculated at each PI coil for each of five different outlet sizes, as a function of depth in column from the initial centre of the free surface (see Fig. 4). Three tendencies of instantaneous vertical velocity were observed. The first tendency for depths ranging from 0 to about 12 cm represented the top of the column. There was a rapid increase in average vertical velocity in this section with increasing depth, for each outlet size, similar to that obtained by Bertho (2003). It appears that the increase of the velocity in this region was due to the decrease of the compactness, which corresponds to the formation of the emptying cone. The second tendency was for depths from about 120 to 820 mm. In this section, the velocity of the tracer varied only with the diameter of outlet. The third tendency was for depths above 820 mm, which represented the region at the bottom of the column and just above the outlet. For the outlet openings of 68.0, 62.5, 54.5 and 44.0 mm diameters, the tracer was accelerated again and the average vertical velocity of the tracer reached its maximum. This was because the tracer particles were released from the bulk of particles to the free air at the outlet. These results are in agreement with the observations reported by Steingart and Evans (2005). In addition, for each outlet, we noted a series of accelerated and decelerated movements of the tracer. These movements were repetitive and similar for each test. The periodic acceleration and deceleration observed in the vertical velocity measurements of the tracer as a function of depth were also observed experimentally in previous studies (Valance & Le Pennec, 1998; Degouet, 2005; Horlüch & Dimon, 2001; Tsai, Losert, Voth, Gollub, 2002). These irregularities of the particle flow are known to cause vibrations in silos, termed as "silos music" (Tejchman, 1998). Fig. 4 shows an increase in the amplitude of the fluctuations of the velocity with the diameter of outlet opening. Fig. 5 depicts the percent variation in velocity for each outlet size. Besides the higher percent variations of velocity in the depth range of 0 to 120 mm as flow initiated, the 62.5 mm opening had an increase in percent variation of velocity from about 300 mm to 65 mm in depth. This phenomenon was generated due to the plug flow behaviour caused by the sudden opening where the profile of the free surface does not evolve (Schulze, 1998) to the chimney-like flow (Watson & Rotter, 1996). The plug flow effect had a direct influence on the vertical velocities of the free surface (Degouet, 2005).

### 3.3 Average mass flow

Table 4 summarizes the average mass flow rates obtained by applying three equations (Eqs. 2, 3, and 5) and using the data from the Table 3 for each outlet size. The power model (Eq. 4) fitted with the data from Eqs. (2) and (3) and using $n = 2.5$ resulted in $R^2 = 0.91$. Because of the similar results obtained by both equations, we used the average results of mass flow rate obtained by the Eqs. (2) and (3) and fitted them with the Beverloo model (Eq. 5). Fitting with the Beverloo model resulted in $R^2 = 0.53$ for $n = 2.5$ and $R^2 = 0.90$ for $n = 2.39$ (see Fig. 6). Thus, the quantitative analysis of the experimental mass flow rate and the diameter of outlet opening in accordance with Beverloo et al. (1961) allowed us to propose a function as given in equation (5) with an exponent value of $n = 2.39$ instead of $n = 2.50$. The gap between the two preceding values of the exponent being $\Delta n = 0.11$ can be further reduced to a value of $\Delta n = 0.09$, if the outlet diameter is 36.5 to 54.5 mm. Within this outlet diameter range, the fit for $n = 2.41$ was $R^2 = 0.95$ while the fit for $n = 2.5$ was $R^2 = 0.66$. The difference $\Delta n = 0.11$ can be translated, firstly by comparing the size of bead ($d$) and the diameter $D$ of the outlet opening. If the $d/D$ (for large outlet openings) is negligible compared to 1.0, the flow rate given by the law of Beverloo et al. (1961) presented in Eq. (5) evolves into the equation

$$Q \cong C_b \rho_a g^{0.5} D^{2.5} \tag{6}$$

which is comparable to Eq. (4) with $n$ = 2.5 ($R^2$=0.91 for Eqs. (2) and (3)). This result coincides with experimental results and previous numerical simulations (Mankoc et al., 2007; Garcimartín et al., 2009; Perge, 2010).

## 4. Conclusions

The PI technique was used to detect a tracer particle within a column (ID = 75 mm) with outlet diameters ranging from 36.5 to 68.0 mm and granular particles of approximately 8 mm diameter. It was possible to determine the longitudinal profile of the vertical velocity and the mass flow rate of particulates. Analysis of the results showed that the vertical velocity (and respective flow rate) was independent of the height of the beads. The parameter which controlled the vertical velocity and the flow rate was the outlet diameter. Within the range of experimental conditions, Eq. (5) (Beverloo et al., 1961) was proposed with an exponent value of $n$ = 2.39 ($R^2$ = 0.90) instead of $n$ = 2.50 ($R^2$ = 0.53) to model mass flow.  Also, the grain flow behaviour can be expressed by Eq. (5) with $n$ = 2.41 ($R^2$ = 0.95) in a range of outlet diameters between 36.5 and 54.5 mm. In summary, the PI measurement of the coupled time-height of a tracer at different points of a granular flow proved to be a reliable system of flow measurement in opaque ducts. In addition, this measurement technique can be used in transparent ducts to provide grain flow measurements inside as well as outside of the surface forming the granular volume.

## References

Andrade, J., Trevino, C., & Medina, A. (1996). Experimental evidence of density fluctuations two-dimensional bins. *Physics Letters A*, 223, 105–110.

Bertho, Y. (2003). Dynamiques d'écoulements gaz-particules en conduite verticale. PhD thesis, Ecole Polytechnique, Paris.

Beverloo, W. A., Leniger, H. A., & van de Velde, J. (1961). The flow of granular solids trough orifices. *Chemical Engineering Science*, 15, 260–269.

Chevoir, F., Prochnow, M., Moucheront, P. da Cruz, F., Bertrand, F., Guilbaud, J–P., Coussot, P., & Roux, J. N. (2001). Dense granular flows in a vertical chute. In Y. Kishino (Ed.), *Powders and Grains 2001* (pp. 399-402). Lisse, Netherlands:  A. A. Balkema.

Chou, C. S., Hsu, J. Y., & Lau, Y. D. (2002). The granular flow in a two dimensional flat bottomed hopper with eccentric discharge. *Physics A*, 308, 46–58.

Crone, R., & Crone, D. (1989). Twin loop treasure seeker. ETI (review British), 42-47. Available at http://www.geotech1.com/pages/metdet/projects/twinloop/twinloop.pdf.

Degouet, C. (2005). Caractérisation de matériaux granulaires et de leurs écoulements dans les silos verticaux : Mise en œuvre d'une méthode d'investigation expérimentale et numérique : Ph.D. thesis, Université de Bretagne Occidentale Brest, France.

Duran, J. (1997). *Sables, poudres et grains. Introduction à la physique des milieux granulaires*. Paris : Eyrolles Sciences, (Chapter 1).

Garcimartín, A., Mankoc, C., Janda, A., Arévalo, R., Pastor, J. M., Zuriguel, I., & Maza, D. (2009). Flow and jamming of granular matter through an orifice. In C. Appert-Rolland, F. Chevoir, P. Gondret, S. Lassarre, J.-P. Lebacque, & M. Schreckenberg (Eds.), *Traffic and granularfFlow 07* (pp. 471-486). Berlin: Springer-Verlag.

Guelle, D., Smith, A., Lewis, A., & Bloodworth, T. (2003). *Metal detector handbook for humanitarian demining*. Luxembourg: Office for Official Publications of the European Communities, (Chapter 4).

Horlüch, S., & Dimon, P. (2001). Grain dynamics in a two-dimensional granular flow. *Physical Review E*, 63(3), 031301.

Jackson, R. (2000). *The dynamics of fluidized particles* (Chap. 7). United Kingdom: Cambridge University Press.

Jaeger, H. M., & Nagel, S. R. (1992). Physics of the granular state. *Science*, 255, 1523–1531.

Le Pennec, T., Ammi, M., Messager, J. C., Truffin, B., Bideau, D., & Garnier, J. (1995). Effect of gravity on mass flow rate in an hour glass. *Powder Technology*, 85, 279–281.

Lubert, M. (2000). Aptitude à l'Ecoulement d'un Milieu Granulaire : Exploitation des Instabilités de cisaillement et Evaluation du Vieillissement. Ph.D. thesis, Ecole des Mines d'Albi, Universite de Provence, France.

Mankoc, C., Janda, A., Arévalo, R., Pastor, J. M., Zuriguel, I., Garcimartín, A., & Maza D. (2007). The flow rate of granular materials through an orifice. *Granular Matter*, 9(6), 407-414.

Medina, A., Andrade, J., & Trevino, C. (1998). Experimental study of the tracer in the granular flow in a 2D silo. *Physics Letters A*, 249, 63-68.

Mitarai, N., & Nori F. (2006). Wet granular materials. *Journal of Advances in Physics,* 55, 1-45.

Ooi, J. Y., & Rotter, J. M. (1998). Flow visualization In C. J. Brown & J. Nielsen (Eds.), *Silos Fundamentals of theory, behaviour and design* (pp. 745-760). London: E & FN Spon.

Ooi, J. Y., Chen, J. F., & Rotter, J. M. (1998). Measurement of solids flows patterns in a gypsum silo. *Powder Technology*, 99, 272–284.

Perge, C. (2010). Contraintes et débit lors de la vidange d'un silo de grains. Stage 2010-2011, Ecole Centrale de Lyon, Université Claude Bernard Lyon1 - INSA Lyon – ENTPE.

Reydellet, G., Rioual, F., & Clément, E. (2000). Granular hydrodynamics and density wave regimes in a vertical chute experiment. *Europhysics Letters*, 51(1), 27–33.

Schulze, D. (1998). Silo quaking. In C. J. Brown, & J. Nielsen (Eds.), *Silos Fundamentals of theory, behavior and design* (pp. 171–182). London: E & FN Spon.

Steingart, D. A., & Evans, J. W. (2005). Measurements of granular flows in two-dimensional hoppers by particle image velocimetry. Part I: Experimental method and results. *Chemical Engineering Science*, 60, 1043-1051.

Stuart, M. (1994). Microcontroller PI Treasure Hunter: Everyday with Practical Electronics, 28–49. UK publisher Wimborne Publishing, Ltd.

Tejchman, J. (1998). Silo quake measurements, a numerical approach and a way for its suppression. *Thin-Walled Structures*, 31, 137–158.

Tsai, J. C., Losert, W., Voth, G. A., & Gollub, J. P. (2002). Two-dimensional granular Poiseuille flow on an incline: multiple dynamical regimes. *Physical Review E*, 65, 011306.

Valance, A., & Le Pennec, T. (1998). Nonlinear dynamics of density waves in granular flows through narrow vertical channels. *European Physical Journal B*, 5(2), 223-229.

Wang, C., Jackson, R., & Sundaresan, S. (1997). Instabilities of fully developed rapid flow of a granular material in a channel. *Journal of Fluid Mechanics*, 342, 179-197.

Watson, G. R., & Rotter, J. M. (1996). A finite element kinematic analysis of planar granular solids flow. *Chemical Engineering Science*, 51(16), 3967-3978.

**Figure Caption**

Fig. 1. **(a)** Experimental device: **C**, column; **CO**, PI coil; **TM**, task manager; **DT**, detector; **TI**, set of timers; **OB**, obturator; **CN**, outlet cone; **MCO**, mechanism controlling the opening of the obturator; **(b)** Schematic diagram of the closed state of the obturator **(c)** Schematic diagram of the opening state of the obturator.

Fig. 2**. (a)** Photo of the experimental device for measuring the path time of the tracer in a bulk of beads: **FF**, feeding funnel; **C**, opaque column; **CO**, PI coil; **TM**; task manager; **TI**, set of timers; **OB**, obturator; **MCO**, mechanism controlling the opening of the obturator; **DT**, detector; **BU**, bucket to collect beads. **(b)** Photo of device to measure the real heights of the detection: **EM**, electromechanical module (electric motor slaved+ converter infrared light into electric pulse); **TSW**, tracer suspended by a wire; **CNW**, counterweight; **GR**, graduated rule; **PC**, pulse counter.

Fig. 3. Change in tracer height in experimental column over time for five different outlet sizes. Tracer was initially placed at the centre of the free surface.

Fig. 4. Instantaneous vertical velocity of the tracer calculated at each PI coil for each of five different outlet sizes, as a function of depth of detection in column from the centre of the free surface.

Fig. 5. Expected percent variation of the relative error of the tracer velocity as a function of the depth of detection and the diameter of the opening of the orifice.

Fig. 6. Predicted average mass flow as function of diameter of outlet orifice

**C**

**CO**

**DT**

**TM**

**OB**

**CN**

**TI**

**M.C.O**

**(a)**

**(b)**

**(c)**

(a)                    (b)

**Height (mm)** vs **Time (s)**
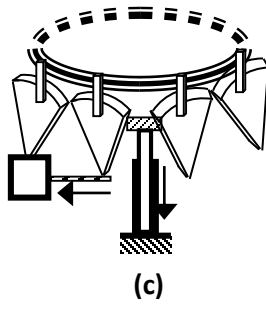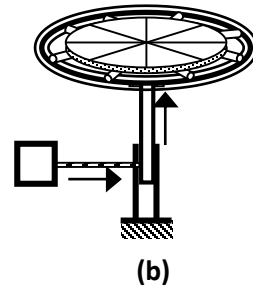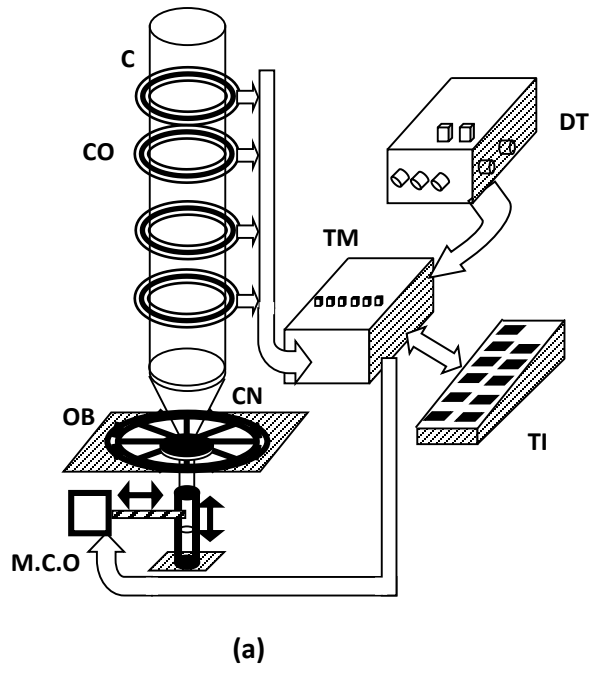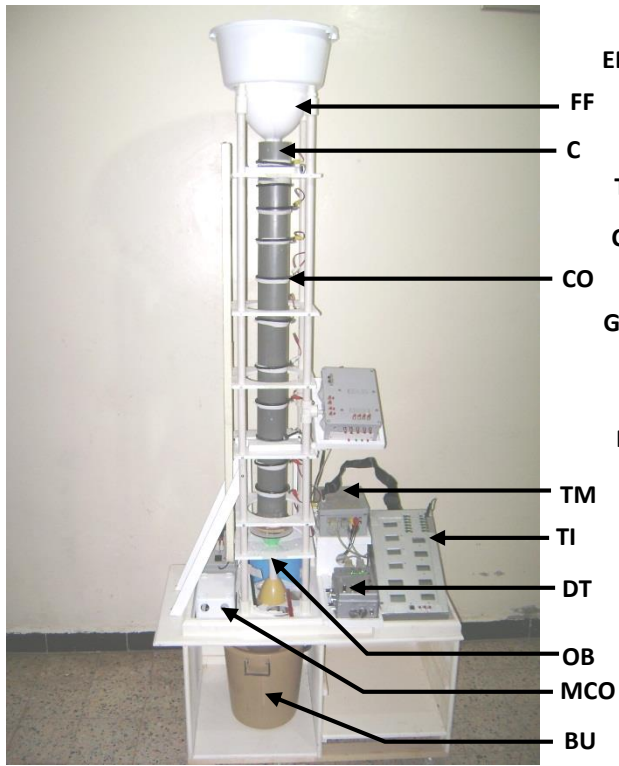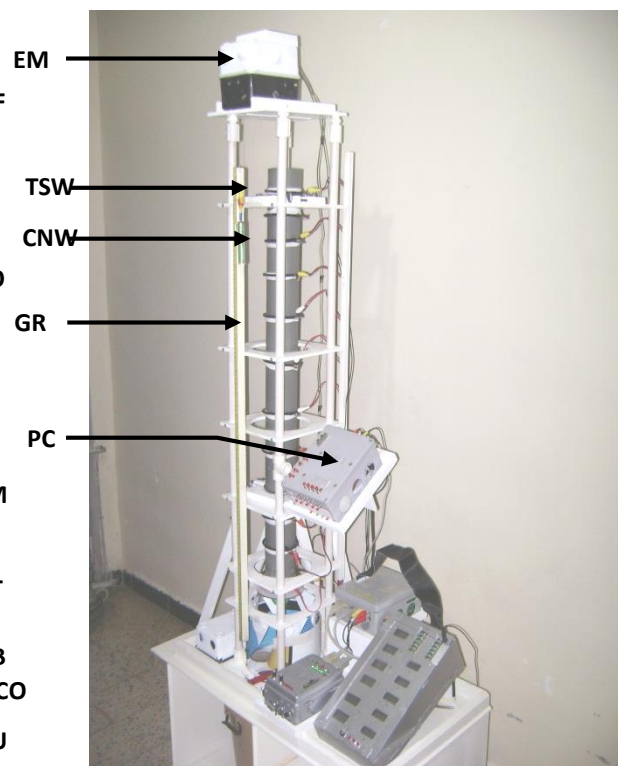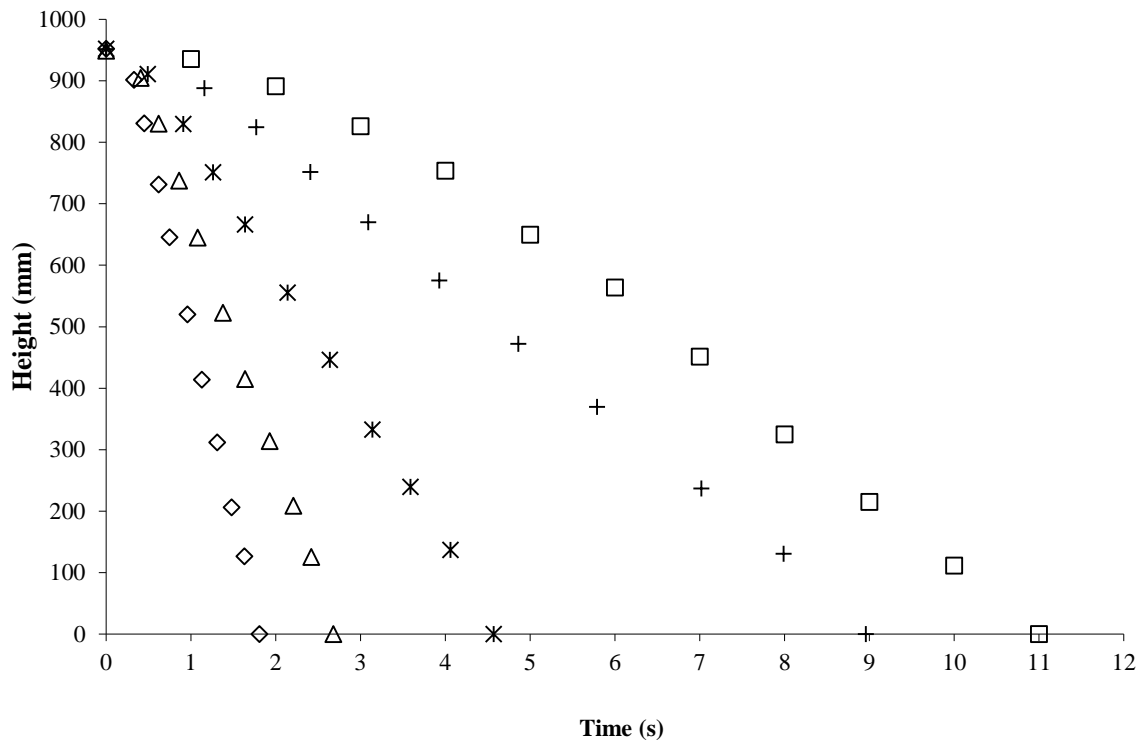
◇ 68.0 mm    △ 62.5 mm    ✳ 54.5 mm    + 44.0 mm    □ 36.5 mm

**Outlet diameter (mm)**

| | Eq. 1 | Eq. 2 | Eq. 5, n = 2.50 | Eq. 5, n = 2.39 |
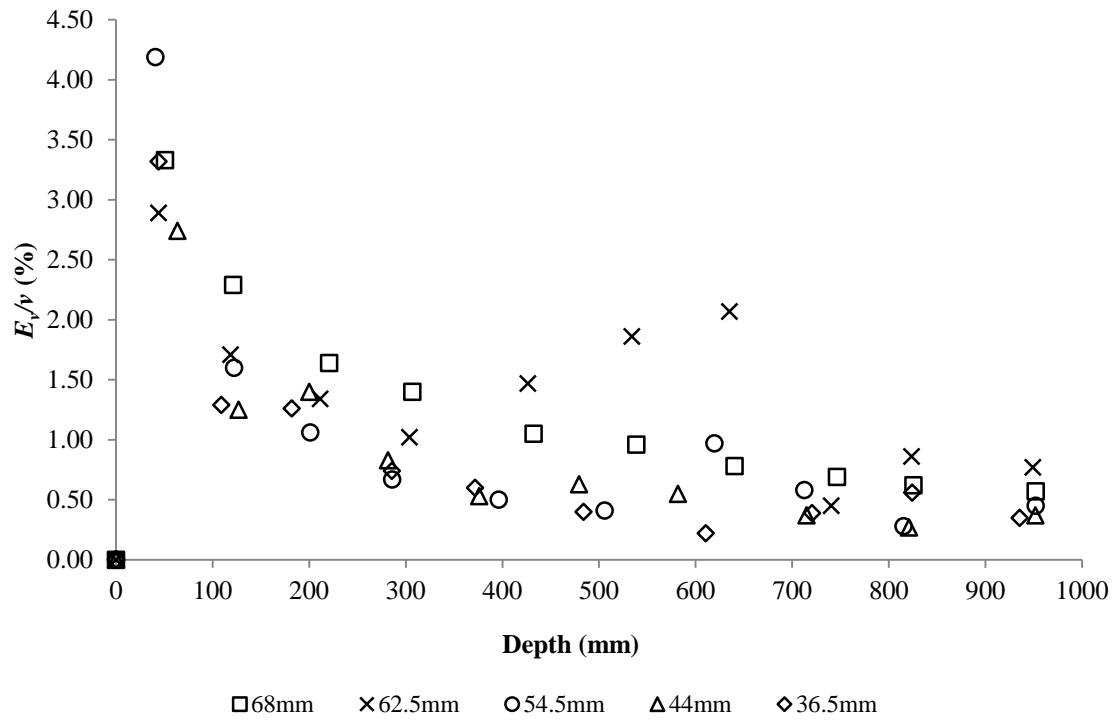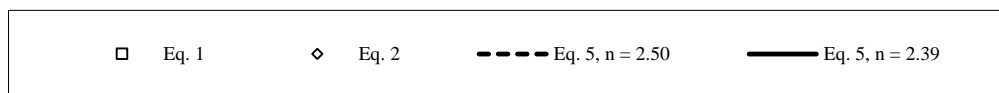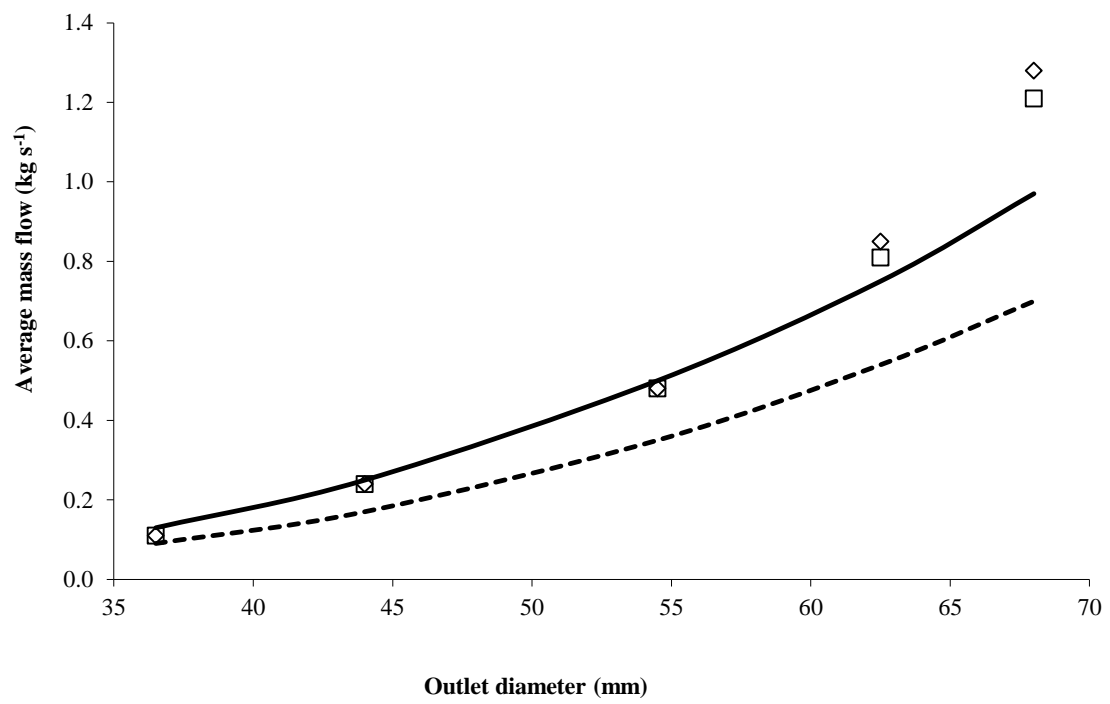
Table 1: Geometric dimensions of the cones used at the outlet.

| Cone | $C_1$ | $C_2$ | $C_3$ | $C_4$ | $C_5$ |
|---|---|---|---|---|---|
| Inside diameter at entry to cone, $D_{Ci}$ (mm) | 75.0 | 75.0 | 75.0 | 75.0 | 75.0 |
| Inside diameter at exit of cone, $D$ (mm) | 36.5 | 44.0 | 54.5 | 62.5 | 68.0 |
| Height of cone, $h_c$ (mm) | 43.4 | 34.5 | 26.3 | 19.0 | 10.2 |

Table 2. Summary of mean elapsed time and standard deviation between start-up timer and each timer corresponding to a PI coil, for each outlet diameter.

| | Column Outlet Diameter (mm) | | | | | | | | | |
| | 36.5 | | 44.0 | | 54.5 | | 62.5 | | 68.0 | |
| Coil | Mean (s) | SD (s) | Mean (s) | SD (s) | Mean (s) | SD (s) | Mean (s) | SD (s) | Mean (s) | SD (s) |
|---|---|---|---|---|---|---|---|---|---|---|
| 1 | 2.09 | 0.15 | 1.16 | 0.07 | 0.49 | 0.03 | 0.41 | 0.03 | 0.33 | 0.02 |
| 2 | 3.49 | 0.10 | 1.77 | 0.05 | 0.91 | 0.03 | 0.62 | 0.02 | 0.45 | 0.02 |
| 3 | 5.01 | 0.11 | 2.41 | 0.06 | 1.26 | 0.03 | 0.86 | 0.02 | 0.62 | 0.02 |
| 4 | 6.94 | 0.10 | 3.09 | 0.04 | 1.64 | 0.03 | 1.08 | 0.02 | 0.75 | 0.02 |
| 5 | 8.66 | 0.12 | 3.93 | 0.04 | 2.14 | 0.03 | 1.38 | 0.04 | 0.96 | 0.03 |
| 6 | 10.92 | 0.10 | 4.86 | 0.06 | 2.64 | 0.03 | 1.64 | 0.06 | 1.13 | 0.02 |
| 7 | 13.65 | 0.08 | 5.79 | 0.07 | 3.14 | 0.06 | 1.93 | 0.08 | 1.31 | 0.02 |
| 8 | 15.82 | 0.09 | 7.02 | 0.04 | 3.59 | 0.05 | 2.21 | 0.03 | 1.48 | 0.02 |
| 9 | 17.77 | 0.19 | 7.99 | 0.05 | 4.06 | 0.03 | 2.42 | 0.04 | 1.63 | 0.02 |
| 10 | 19.71 | 0.14 | 8.96 | 0.06 | 4.57 | 0.05 | 2.68 | 0.04 | 1.81 | 0.02 |

Table 3: Summary of kinematic and geometric parameters for each outlet diameter.

| Outlet Diameter, $D$ (mm) | Mean Velocity of Tracer, $V_{mean} \pm E_v$ (m s$^{-1}$) | Initial depth of particles, $h_{max} \pm E_h$ (mm) | Time to empty, $t_{max} \pm E_t$ (s) |
|---|---|---|---|
| 68.0 | 0.5602 ± 0.0064 | 952.2 ± 1.0 | 1.81 ± 0.01 |
| 62.5 | 0.3691 ± 0.0049 | 949.0 ± 1.5 | 2.68 ± 0.02 |
| 54.5 | 0.2078 ± 0.0016 | 952.0 ± 1.0 | 4.57 ± 0.02 |
| 44.0 | 0.1052 ± 0.0008 | 951.6 ± 1.6 | 8.96 ± 0.03 |
| 36.5 | 0.0474 ± 0.0003 | 935.4 ± 1.6 | 19.71 ± 0.06 |

Table 4: Average mass flow for each equation for each outlet diameter.

| Outlet Diameter, D (mm) | Mean Mass Flow, $Q \pm E_Q$ (kg s$^{-1}$) | | Equation (5) | |
|---|---|---|---|---|
| | Eq. (2) | Eq. (3) | $n$=2.50 | $n$=2.39 |
| 68.0 | 1.21 ± 0.01 | 1.28 ± 0.01 | 0.70 ± 0.01 | 0.97 ± 0.01 |
| 62.5 | 0.81 ± 0.01 | 0.85 ± 0.01 | 0.54 ± 0.01 | 0.75 ± 0.01 |
| 54.5 | 0.48 ± 0.00 | 0.48 ± 0.00 | 0.35 ± 0.01 | 0.50 ± 0.01 |
| 44.0 | 0.24 ± 0.00 | 0.24 ± 0.00 | 0.17 ± 0.02 | 0.25 ± 0.02 |
| 36.5 | 0.11 ± 0.00 | 0.11 ± 0.00 | 0.09 ± 0.02 | 0.13 ± 0.02 |